Propagation Characterization for an Indoor Wireless Sensor Network with Energy Harvesting

P. H. Krohling Almeida, L. C. Nogueira, E. E. Benitez Olivo, and D. P. Moya Osorio

***Abstract*— This paper carries out an experiment-based channel characterization for a wireless sensor network based on the development kit TI eZ430-RF2500-SEH, which operates with solar energy harvesting. The channel model was obtained from measurements of the received signal strength (RSS) in an indoor environment. This model is tested through a coverage sensor application, and the energy management of the device is also investigated.**

***Keywords*— Wireless sensor networks, energy harvesting, channel characterization.**

I. Introduction

In the *Internet of Things* (IoT), a myriad of devices, provided of sensors, will interact in an autonomous and smart manner. Thus, wireless sensor networks (WSNs) will be an essential part of the IoT, as this kind of networks can be widely used to monitor and collect data from the environment, thereby enabling different services and applications. WSNs have been investigated in the most diverse scenarios [1], [2]. For instance, in [1], a two slope, log-normal path loss near ground outdoor model is characterized for a WSN at 868 MHz. In [2], the authors proposed a statistical channel model for a suburban environment, where the multipath and shadowing phenomena are predominant. However, the energy resources in WSNs represent a challenging issue due to the current dependency on batteries. Therefore, energy harvesting techniques have proved to be a promising solution for WSNs [3]. In this paper, an experiment-based path loss model for a WSN based on the TI eZ430-RF2500-SEH kit, which operates with solar energy harvesting, is obtained through measurements of RSS in an indoor environment. This model is tested through a coverage sensor application. In addition, the energy management of the WSN is investigated.

The rest of this paper is organized as follows: section II presents the theory used; section III presents the procedure to measurements and the model obtained; section IV presents the effectiveness of the model in a coverage sensor application; section V presents the module's power consumption; finally section VI presents the conclusions of this work.

II. Channel Modeling

In this paper, we consider two large-scale models, which are described next.

A. Log-Distance Path loss Model

This model considers that the average received signal power shows a logarithmic decrease with the distance between transmitter and receiver, which is expressed as

$$P_L[\mathrm{dB}] = P_L(d_0) + 10n\log\left(\frac{d}{d_0}\right), \qquad (1)$$

P. H. Krohling Almeida, L. C. Nogueira, and D. P. Moya Osorio are with the Federal University of São Carlos (UFSCar), São Carlos-SP, Brazil, E-mails: pdrkrohl@gmail.com, leonardongr13@gmail.com, and dianamoya@ufscar.br.

E. E. Benitez Olivo is with São Paulo State University (UNESP), Campus of São João da Boa Vista, São João da Boa Vista-SP, Brazil, E-mail: edgar.olivo@unesp.br.

This work was supported by FAPESP (Procs. N^o 2017/09389-9 and 2017/07320-1).

where, $P_L(d_0)$ is the path loss at the reference distance d_0, n is the path loss exponent, and d is the distance between transmitter and receiver. Therefore, the received power can be obtained as $P_r[\mathrm{dBm}] = P_t[\mathrm{dBm}] - P_L[\mathrm{dB}]$, where $P_t[\mathrm{dBm}]$ is the transmit power.

Then, for a given scenario, the path loss exponent n can be empirically determined from channel measurements by minimizing the square mean error between the predicted and measured path loss. Hence, the error can be determined as

$$E(n) = \sum_{i=1}^{k}\left[P_{Lm_i} - P_{Lp_i}\right]^2, \qquad (2)$$

where P_{Lm} is the average measured path loss, P_{Lp} is the predicted path loss at each point obtained as in (1), and k is the total number of points. By substituting (1) into (2) and differentiating the result in order to minimize the error, the path loss exponent is obtained as

$$n = \frac{\sum_{i=1}^{k}\left[P_{Lm_i} - P_L(d_0)\right]\log\left(\frac{d_i}{d_0}\right)}{\sum_{i=1}^{k}\left[10\log\left(\frac{d_i}{d_0}\right)\right]\log\left(\frac{d_i}{d_0}\right)}. \qquad (3)$$

B. Log-Normal Shadowing

While the log-distance model is deterministic, the random effect due to objects near to the receiver can be characterized using the log-normal shadowing model [4]. This model includes a random variable (RV) X_σ to the log-distance model given in (1), which follows a Gaussian distribution of zero mean and standard deviation σ. Therefore, to empirically determine this model, once the value of n is obtained as described in the above section, the log-distance model is used as the expected value, and the measurement points are projected over that value. Then, σ is calculated as

$$\sigma[\mathrm{dB}] = \sqrt{\sum_{i=1}^{N}\frac{(X_i-\mu)^2}{N}}, \qquad (4)$$

where X_i are the projections, μ is the mean of the distribution (0 by considering the path loss model as reference), and N is the number of measurements.

III. Methodology

To predict the channel propagation model, measurements of RSS at the anchor node (receiver) of the signal transmitted from a mobile node (transmitter) were taken on 5 different points in order to eliminate both temporal and spacial variation of the channel. To eliminate the temporal variation, at each point, 20 measurements were taken in intervals of 30 min. Moreover, to eliminate the spacial variation, measurements were taken in others 10 points separated 10 cm for each original point. Then, the average RSS for each point is calculated by finding the expected value of all measurements. Thus, from (3) and (4), the experimental values for the corresponding model parameters were obtained as $n = 1.0028$ and $\sigma = 0.3372$.

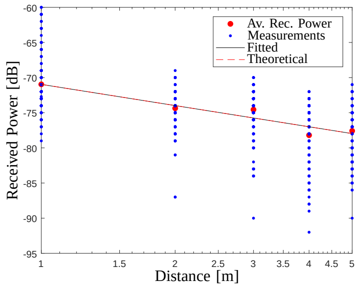

Fig. 1. Theoretic and adjusted curves from measurements points.

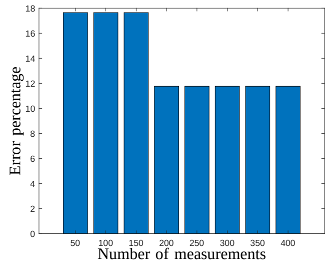

Fig. 2. Error in evaluation of coverage area by number of measurements.

Fig. 1 shows the curve attained by replacing n as obtained in (1), and the fitted curve obtained in Matlab from the measured points, where it was considered $P_L(d_0) = 70.96$ dB at $d_0 = 1$ m. Note that the theoretical and fitted curves are almost overlapping, thus verifying the accuracy of the theoretical calculations.

IV. Coverage Sensor

In order to verify our model, an application for sensors that predicts if a transmitter is inside a coverage area was employed. For that purpose, measurements of RSS were taken at 17 different distances from 1 to 5 m, since the coverage area was set to 3 m. Then, the path loss model determined in Section III was used to predict whether the transmitter is inside or outside the coverage area. Fig. 2 shows the error percentage as a function of the number of measurements. It is observed that, for 200 or more measurements (≈ 30 min), an error of less than 12% is attained.

V. Energy Management

The Solar Energy Harvesting Module (SEH-01) of the TI eZ430-RF2500-SEH kit is based on a photovoltaic cell responsible for converting the incident light into electrical energy. Then, a boost converter is used to increase the voltage to a proper level to charge the EnerChip EH CBC5300 inner batteries on the SEH-01. The device power management was observed by testing its behavior whenever the photovoltaic cell or the batteries EH CBC5300 act as the main power supply in two distinct experiments as follows.

1) EnerChip batteries: The first experiment aims to demonstrate the autonomy of the EnerChip batteries whenever the photovoltaic cell is not able to provide enough energy for the proper operation of the device. For such evaluation, the SEH-01 was supplied by a constant luminescent source of light for 30 minutes, then the mobile node was disconnected from the photovoltaic cell and the EnerChip took its place, ensuring the voltage supply for the microcontroller. Then, periodical transmissions were performed until the batteries were discharged. This process was repeated for all the available time interval settings. It was observed that the device was capable of reaching over 12 hours for the largest period of inactivity available (≈ 4 min) and almost 37 min for the shortest period (≈ 5 s), as shown on Tab. I.

TABLE I

Comparison between the EnerChip battery duration and tested transmission intervals

	Inteval between transmissions (s)					
	5	10	20	40	120	240
Duration (s)	2189	3884	7497	15765	29049	45935

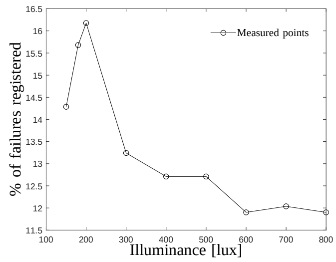

Fig. 3. Registered faults percentual according to the incident illuminance.

2) Luminous Influence: The second experiment aims to analyze the luminous influence over the device operation for distinct levels of luminescence. For this purpose, the device was exposed to a controlled constant light source and 570 measurements were recorded. Then, the elapsed time was analyzed between measurements with a time interval of 5 s. In this way, intervals greater than 5 s were computed as transmission failures, thus a failure occurrence probability was obtained. Note from Fig. 3 that for lower values of illuminance, the device presents more instabilities. However, from 300 lux, the failure rate is below 14%.

VI. Conclusions

In this paper, an experiment-based channel model for a WSN based on the TI eZ430-RF2500-SEH kit, which operates with solar energy harvesting, was obtained through measurements of the received signal strength in an indoor environment. The model was tested through a coverage sensor application. It was observed that the sensor attains almost 90% of accuracy for a number of measurements, greater than 200. Thus, this is not suitable for delay-constrained applications, but useful for many other applications that doesn't require precision, immediate feedback or have few resources. It was also determined that, under insufficient light conditions, the WSN attains up to 12 hours of autonomy for a high load of transmissions.

References

[1] A. Martinez-Sala et al., "An accurate radio channel model for wireless sensor networks simulation," in *Journal of Communications and Networks*, vol. 7, no. 4, pp. 401-407, Dec. 2005.

[2] E. Greenberg and A. Sheinberg, "Statistical channel model for wireless'sensor networks deployment in suburban environment", in *Proc. of the 9th European Conference on Antennas and Propagation*, May 2015, pp. 1-5.

[3] K. Z. Panatik et al., "Energy harvesting in wireless sensor networks: A survey", *IEEE 3rd International Symposium on Telecommunication Technologies*, Kuala Lumpur, 2016, pp. 53-58.

[4] T. Rappaport, *Wireless Communications: Principles and Practice*, 2nd ed.Upper Saddle River, NJ, USA: Prentice Hall PTR, 2001.